

Electrochemical modulation of sickle cell haemoglobin polymerisation†

Zeshan Iqbal,^a Rachel McKendry,^b Michael Horton^b and Daren J. Caruana^{*a}

Received 14th September 2006, Accepted 2nd November 2006

First published as an Advance Article on the web 17th November 2006

DOI: 10.1039/b613381a

Sickle cell haemoglobin (HbS) differs from normal haemoglobin by a single amino acid in its β chain. This amino acid replacement, from glutamic acid to valine, causes polymerisation of proteins into defined long insoluble fibres with a typical diameter of 21.5 nm. The polymerisation is triggered by the formation of deoxyhaemoglobin (deoxyHb) from oxyhaemoglobin (oxyHb) in low oxygen partial pressures, which results in a conformational change in the secondary structure of the protein. We describe an electrochemical method to modulate the oxygen concentration in an optically transparent thin layer cell to produce deoxyhaemoglobin whilst monitoring the extent of polymerisation using turbidity measurements. The oxygen is depleted in the vicinity of the electrode and triggers the polymerisation. The kinetics of polymerisation were investigated using a model for fibrillogenesis describing a two-step process of nucleation followed by elongation. Rate constants describing the nucleation and growth at monomer concentration of 300 mg cm^{-3} ($4.65 \times 10^{-3} \text{ M}$) were determined to be $9.45 (\pm 0.08) \times 10^{-6} \text{ s}^{-1}$ and $1.22 (\pm 0.03) \times 10^{-3} \text{ s}^{-1}$ respectively, showing that nucleation was far slower than the growth. A similar difference between the rate constants for the nucleation ($2.99 (\pm 0.4) \times 10^{-8} \text{ s}^{-1}$) and growth ($1.08 (\pm 0.2) \times 10^{-3} \text{ s}^{-1}$) was seen at monomer concentration of 50 mg cm^{-3} ($7.75 \times 10^{-4} \text{ M}$). These results show that nucleation was monomer concentration dependent; however growth was largely independent of monomer concentration. In this study we present a methodology that may be used as a screening method for substances that effect the fibre nucleation and or growth that could be valuable to the pharmaceutical industry for treating sickle cell disease.

1. Introduction

The clinical features of sickle cell disease, a genetic disorder of the blood in which the red blood cells curve into a sickle shape, are directly dependent on polymerisation and gelation of deoxygenated haemoglobin S (HbS) molecules. HbS is a single point genetic mutation of adult haemoglobin (HbA) that results in a hydrophobic valine (Val) residue replacing hydrophilic glutamic acid (Glu) in the sixth codon of each β chain.^{1,2} Consequently, HbS monomers when in the deoxygenated or T (tense) allosteric state interact and associate with hydrophobic pockets, formed by $\beta 85$ phenylamine (Phe) and $\beta 88$ leucine (Leu) residues on different tetramers, to produce double strands, which polymerise into long stiff insoluble rod-like fibres of 21.5 nm diameter. The fibres consist of six double strands wrapped around a central strand in the form of a twisted rope with a pitch of 270 nm.³ Subsequently, under physiological conditions during transit from fully oxygenated arterial blood to the relatively hypoxic venous circulation, the fibres fill the red cell and form non-covalent cross-links to create a gel causing the red cell to become rigid and deformed; as a result, sickled cells block blood flow in vascular capillaries.

Sickle cell disease is an international health problem affecting millions of people around the world. It is most common in East and Central Africa where as many as 25% of the people have the sickle cell trait and 1–2% of all babies are born with a form of the disease.⁴ The kinetics of fibre formation and polymerisation play a central role in understanding the physical chemistry of HbS polymerisation as well as the pathophysiology of sickle cell anaemia. A full understanding of this process should improve therapeutic strategies for this common, and frequently disabling, genetic disorder.

The double nucleation mechanism of Ferrone *et al.*,⁵ postulates that polymer formation is the result of two types of nucleation: homogeneous and heterogeneous. In homogeneous nucleation, aggregation of HbS monomers occurs in the bulk until the aggregate reaches a certain size, termed the critical nucleus. The sequential addition of free monomers is thermodynamically unfavourable, initially as substantial loss of translational and rotational freedom of the monomer is only partially compensated for by the entropy gain from the centre of mass and torsional vibrations of the molecules in a polymer lattice. This nucleation step is characterised by a delay time accounted for by the time taken to form the critical nuclei.

On the other hand, heterogeneous nucleation involves nucleation on the surface of pre-existing polymers as well as growth of polymers. As more polymers form, the available surface area and thus the number of available sites for heterogeneous nucleation increase with time. As a result, there is a continuous increase in the rate of heterogeneous nucleation providing an explanation for the exponential growth observed in the progress curves.

^aDepartment of Chemistry, University College London, 20 Gordon St., London, UK WC1H 0AJ

^bLondon Centre for Nanotechnology, 17–19 Gordon St, London, UK WC1H 0AH

† Electronic supplementary information (ESI) available: Film clip of the growth of sickle cell haemoglobin (HbS) fibres on the surface of a 100 μm diameter wire electrode. See DOI: 10.1039/b613381a

The key to HbS polymerisation, however, is the deoxygenated, or T, state of HbS as exposure of the hydrophobic pocket, through which fibre formation is initiated, only occurs in this state.⁶ Experimentally, three methods have been used to convert oxy- to deoxyhaemoglobin. The most commonly employed chemical reagent for the reduction of oxygen (O₂) is sodium dithionite, a reducing agent that acts as a scavenger of residual O₂. Although this method removes O₂ rapidly and completely, the production of hydrogen peroxide (H₂O₂), which is an intermediate of the reaction, is potentially deleterious to the structure of the haemoglobin molecule. The other methods involve the physical removal of O₂, and this is performed either by passing an O₂ free inert gas over the solution or by carbon monoxide (CO) saturation in an anaerobic environment. The latter involves exposure to CO in a glove box which causes HbS molecules to lose oxygen and bind CO.

This study demonstrates a novel technique for the removal of O₂ from haemoglobin—electrochemical reduction at a conducting electrode surface as a tool to study the nucleation and growth of HbS aggregation. The electrochemical reduction of O₂ at metal surfaces is a complex multi-electron process where O₂ is reduced either directly to water or to intermediate H₂O₂, which is itself subsequently decomposed on the electrode or desorbed into the bulk solution in a number of steps.⁷ However, although the reduction reaction involves a number of intermediates in a complex reaction pathway, electrochemistry nevertheless provides a simple, rapid and controllable approach to the complete deoxygenation of solution *in situ*, whilst simultaneously avoiding lengthy preparation times as only reduction at the surface is required.

Much of the published literature on nucleation and growth of HbS and its kinetics has focussed on the polymerisation of HbS in solution, and therefore largely focussed on homogeneous rather than heterogeneous nucleation (see Eaton and Hofrichter for a review⁸), with little emphasis on nucleation and growth on artificial surfaces or at a conducting surface. This is the first study in which electrochemical deoxygenation has been coupled with HbS to investigate rates and dynamics of nucleation and growth at gold (Au) electrodes. This was accomplished using a custom-built thin layer cell fabricated to perform electrochemical techniques coupled with optical microscopy and UV-visible spectroscopy.

2. Experimental

2.1 Materials

HbS and HbA were purchased from Sigma chemical company (Poole, UK) and used as supplied. The supporting electrolyte was 1.5 M (pH 7.0) phosphate buffer solution which was prepared by mixing stock solutions of dihydrogen potassium phosphate and dipotassium hydrogen phosphate (Avocado, UK) to achieve a solution with pH 7.0. Sodium chloride (NaCl) was obtained from BDH AnalaR. Other chemicals were of analytical reagent grade. De-ionised water (Millipore Milli-Q gradient[®], <0.05 S cm⁻²) was used for all solutions.

The electrodes were Au micro-mesh (aperture size 0.25 mm, plain weave wire diameter 0.060 mm, 82 grids per inch, 99.99% purity), Au wire (diameter 0.1 mm, hard temper, 99.99% purity), Pt wire (diameter 0.1 mm, hard temper,

99.99% purity), silver (Ag) wire (grade 1, diameter 0.025 mm). All were obtained from Advent Research Materials Ltd, Oxford or Johnson Matthey, Cambridge.

2.2 Instrumentation

Electrochemistry techniques, specifically chronoamperometry and cyclic voltammetry, were carried out in a conventional three electrode system comprising a counter, working and reference electrodes connected to a potentiostat (μ Autolab Type II, Eco Chemie B.V. supplied by Windsor Scientific Ltd, UK), controlled by GPES software (version 4.7, Eco Chemie B. V. Utrecht, Netherlands). In the three-electrode system a Au micro-mesh optically transparent electrode (OTE) was used as the working electrode, a Pt coil served as the auxiliary electrode whilst all potentials were given *versus* the quasi-reference electrode (Ag/AgCl).

An optical microscope (Jenalab; Carl Zeiss, Germany) connected to a video camera (TK-1085E; JVC, Japan) with PC data collection (Presto Video Works, ver. 4.1, rev. 6; Newsoft Technology Corp, Taiwan) was used for image collection and processing. Images were analysed using Presto Video Works PC data collection software and CorelDraw (ver. 8.232).

Ultraviolet and visible absorption spectra were recorded with an Agilent 8453 UV-visible spectrophotometer (Agilent Technologies) on plain glass microscope slides (0.80 mm \times 1.00 mm thick) using UV-visible ChemStation software (rev. A, 09. 01, Agilent Technologies) in kinetic mode (*i.e.* spectra acquired at regular or increasing time intervals over a period of time). The spectrophotometer experiments run time ranged from 1000 to 4500 s with spectra being recorded at 10 s intervals. The wavelength acquisition range was from 200–1100 nm and time traces at 600, 650, 700 and 800 nm were monitored. The temperature was maintained and controlled with the use of a small peltier device (Thermo Electric cooler type DT1069; Marlow Industries Inc., USA) and measured with a home-made thermocouple.

2.3 Construction of thin layer electrochemical cell

A robust and easily constructed thin-layer cell was designed specifically for optical and spectroelectrochemical measurements. Fig. 1 shows a schematic representation of this cell.

A conventional glass microscope slide and three electrodes—Au micro-mesh (3.0 mm by 4.0 mm), 100 μ m diameter Pt wire with a length of >5 cm serving as the counter electrode and 25 μ m Ag wire reference electrode—were connected to copper electrical wires using silver conductive paint (RS, UK). The connection was covered with epoxy resin (RS, UK) to provide stability as well as to provide an impervious and non-conductive layer (Fig. 1). A coverslip was placed on top of the electrodes and one edge of the coverslip was fixed in position by carefully seeping epoxy resin into the space between the coverslip and electrode and then applying pressure to produce a thin-layer of typical total volume of 50 μ l \pm 10 μ l (measured by the volume of solution required to completely fill the cell).

For the spectroscopy experiments, the entire microscope slide, except for a small window on the Au micro-mesh electrode (1.0 mm by 1.5 mm), was blanked from the light

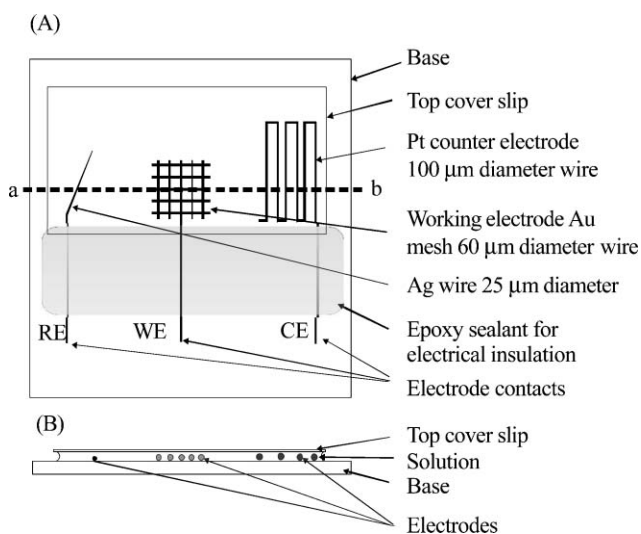


Fig. 1 Schematic representations of the thin layer electrochemical cell used in this work. (A) A plan view showing arrangement of the Au mesh working electrode, 0.1 mm Pt wire counter electrode and 0.025 mm Ag wire, which was electrochemically oxidised to form the reference electrode. (B) A cross section through a–b. Not to scale.

beam. All materials used in the fabrication of the cell were thoroughly cleaned prior to its construction using acetone.

2.4 Procedure

The cell was cleaned by soaking in pure water and then using medical wipes (Kimberley-Clarke, UK) to draw the solution out. The electrodes were electrochemically cleaned by cycling in 0.1 M sulfuric acid until there was no further change in the voltammetric response. Hb protein was dissolved in a solution containing both 1.5 M phosphate buffer (pH 7.0), and 0.5 M sodium chloride. High molarity phosphate buffer and sodium chloride were used to increase the ionic strength and thus increase conductivity of the solution. The high ionic strength also provided a salting out effect for solubility purposes. 50 μl of the Hb solution was pipetted under the coverslip and capillary action ensured that all the electrodes were immersed in the solution. All solutions were used within a day of their preparation. Deoxygenation of Hb solution was performed electrochemically, and in experiments where electrochemistry was not performed, solutions of phosphate buffer were thoroughly degassed with a continuous supply of argon prior to the start of the experiment and during.

A potentiostat was coupled with the optical microscope and UV-visible spectrophotometer so that images of the electrodes and spectra could be taken *in situ*. Cyclic voltammetry of the background solution of 1.5 M pH 7.0 phosphate buffer and 0.5 M NaCl was recorded before every experiment. *In situ* deoxygenation was performed by electrochemical reduction at the electrode ($E = -0.55$ V versus the quasi-reference electrode) using chronoamperometry methods, the time of the experiments varying from 1000 to 6500 s. For cyclic voltammetry, the applied potential was scanned from +0.5 to -0.8 V at a rate of 0.025 V s^{-1} versus quasi-reference electrode. Cyclic voltammograms were taken at the beginning and end of each of the *in situ* electrochemical experiments, Fig. 2.

3. Results and discussion

3.1 Optimisation of thin layer electrochemical cell

A thin-layer cell was fabricated to perform electrochemical measurements, specifically O_2 reduction, on a small volume of Hb and to subsequently monitor ensuing effects on protein aggregation. The essential attributes of this cell were its transparency, enabling physical or structural changes occurring in the solution to be followed, and the capacity to perform electrochemistry in a small volume of oxygenated HbS solution (*i.e.* as a thin layer). The micro-mesh geometry of the working electrode provided an efficient arrangement for oxygen depletion within the thin layer electrochemical cell.

The electrochemical cell incorporating an optically transparent gold micro-mesh electrode was used in tandem with an optical microscope and the UV-visible spectrophotometer to monitor HbS polymerisation at the electrode surface and results showed growth of protein aggregates at the working electrode.

Complete deoxygenation was confirmed electrochemically by comparing the minimum charge needed to remove all O_2 from a cell of total volume 50 μl air-saturated Hb solution, calculated to be 1.93×10^{-3} C, with the experimentally obtained value of 1.00×10^{-2} C passed over a period of 4500 s. Cyclic voltammetry of the solution, performed after chronoamperometry, also showed the absence of the O_2 present in the HbS solution at the start of the experiment, as illustrated in Fig. 2.

Absorption spectroscopy was used to ascertain whether conversion of the oxyHbS to deoxyHbS had occurred. It was important to demonstrate the R to T state flip spectroscopically, as exposure of the hydrophobic pocket by which HbS molecules aggregate only occurs in the T state. Fig. 3 shows the *in situ* electrochemical conversion of oxygenated HbS to its deoxygenated form at a Au micro-mesh electrode. In this particular experiment a 10 mg cm^{-3} HbS, dissolved in a salt solution containing 1.5 M potassium phosphate buffer and 0.5 M NaCl, was used and the electrode was held at -0.55 V for 1000 s. Characteristic peaks at wavelengths 540 nm and 580 nm seen at 0 s indicated the presence of oxygenated haemoglobin,⁹ whilst the depletion of oxygen through

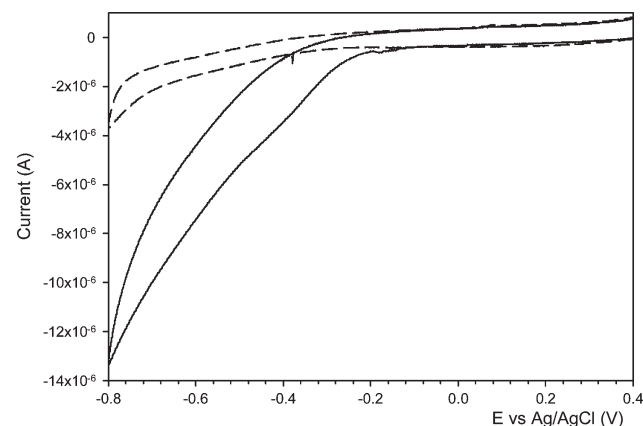


Fig. 2 Cyclic voltammogram of HbS solution before (—) and after (---) reduction of oxygen.

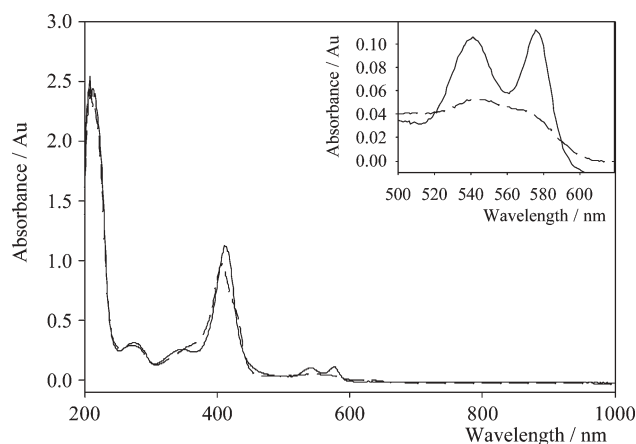
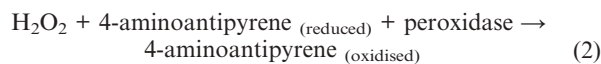
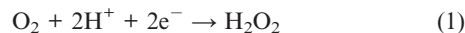


Fig. 3 *In situ* spectroelectrochemistry experiment showing the conversion of oxygenated HbS to deoxygenated HbS at the working electrode, before electrochemical depletion of oxygen (—) and after 1000 s (---). The inset shows the absorbance between 500 to 620 nm for the same spectra. Experiment conditions: HbS concentration 10 mg cm^{-3} ; 1.5 M pH 7.0 phosphate buffer; 0.5 M NaCl; $E = -0.55 \text{ V}$ vs. Ag/AgCl for 1000 s.

potential-step chronoamperometry allowed the formation of T state haemoglobin, characterised by the replacement of the two peaks by a single broad peak at $\sim 560 \text{ nm}$ (dotted line in inset of Fig. 3). This conversion occurred after less than 200 s.

As described earlier, the O_2 reduction reaction at gold is a complex multi-electron process involving different reaction intermediates, with O_2 either being electrochemically reduced directly to water ($\text{O}_2 + 4\text{H}^+ + 4\text{e}^- \rightarrow 2\text{H}_2\text{O}$) or *via* the intermediate H_2O_2 .^{10,11} It was paramount therefore that the oxygen reduction reaction proceeded to completion to avoid any production of H_2O_2 , which can cause Hb degradation and haem loss. The production of H_2O_2 in the HbS solution during the course of the reduction experiment was assayed by a

spectrophotometric technique based on an enzyme linked detection system first described by Barham and Trinder in 1972.¹² The reactions involved are as follows:



Any H_2O_2 formed during electrochemical reaction (1) is reduced by horseradish oxidase which in turn oxidises 4-aminoantipyrene, the reduced acceptor, to produce a chromophore.

The rate at which this chromophore appeared was monitored at 520 nm and each assay was carried out in the thin-layer electrochemical cell both in the background salt solution and in the HbS solution at varying experimental times. The detection limit of this assay was estimated, in a homogenous cell to be $1 \times 10^{-7} \text{ M}$. All assays confirmed that there was no detectable H_2O_2 formation (data not shown).

Furthermore, the production of any OH^- ions locally at the working electrode as a result of the reduction of O_2 , albeit very little as O_2 depletion occurs mainly at the start of the experiment, was minimised by the high buffering capacity.

3.2 Growth of HbS fibrous structures

Fig. 4 shows the morphology of the micro-mesh working electrode and surrounding solution at different time intervals when a solution of HbS was electrochemically deoxygenated (supplementary information is available showing a brief film clip of the growth of protein fibres†). At time = 0 s the Au electrode was bare but at time = 1458 s the first formation of ‘globular structures’ at the electrode was seen (Fig. 4b) and these subsequently grew as the experiment proceeded (Fig. 4c). The time taken for the structures to appear was dependent on the rate of deoxygenation and rate of nucleation of aggregation.

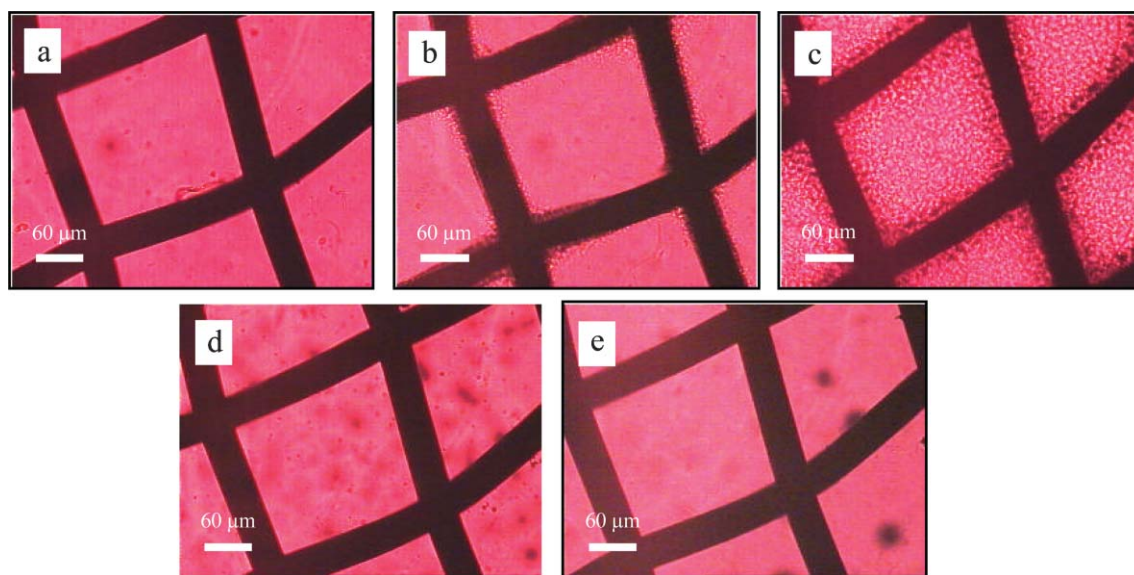


Fig. 4 Optical microscopy images showing HbS fibre growth and the control HbA on Au micromesh working electrode. Experiment conditions: HbS concentration 300 mg cm^{-3} ; 1.5 M pH 7.0 phosphate buffer; 0.5 M NaCl; $E = -0.55 \text{ V}$ versus Ag/AgCl for 4500 s. (a) HbS at 0 s; (b) HbS at 1458 s; (c) HbS at 3327 s; (d) HbA at 0 s; (e) HbA at 4500 s.

Control experiments consisted of substituting HbA for HbS under the same electrochemical conditions in the thin-layer cell. Once O₂ was removed, there was no aggregation of HbA observed on or near the micro-mesh at the end of an experiment over a period of 4500 s, Fig. 4c versus Fig. 4e. The only difference between HbA and HbS is a single amino acid (β 6 Glu \rightarrow Val); HbA monomers do not aggregate even though exposure of the hydrophobic pocket occurs in HbA when in the T allosteric state as charge and size effects prevent β 6 Glu from binding. Furthermore, aggregated structures whose growth had been modulated electrochemically were also seen to disappear once the potential had been switched to open circuit and O₂ had been allowed back into the cell. This reversibility displayed upon reoxygenation is not only specific to our system but also occurs physiologically in the blood vascular system.¹³ Therefore any differences seen in the results from experiments using HbS and HbA are directly attributable to this single amino acid variation. This provided the most compelling evidence that these structures seen on the electrode were due to HbS polymerisation and higher order aggregated structures and not as a result of other factors, such as salt precipitation.

A high molarity phosphate buffer was used (buffer of molarity lower than 1.5 M did not produce any aggregation) and, importantly, NaCl was added to increase the ionic strength and thus conductivity of the solution for electrochemistry. These measures decreased the delay times of nucleation and increased the growth rate through an increase of factors which affect polymer formation and hence improved experimental reproducibility. Ionic strength and salt type have been shown previously to influence aggregation and growth of HbS fibres in other experimental systems.¹⁴

In vivo the Hb concentration per red blood cell (MCHC) is 320–360 mg cm⁻³¹⁵ and the ionic strength of blood plasma is 0.16 M.¹⁶ The choice of 300 mg cm⁻³ as the protein concentration allows a direct comparison to be made with polymerisation *in vivo*. However, a system where lower ionic strength solution can be used still needs to be developed, possibly by increasing the protein concentration or using electrodes where the O₂ reducing capacity is far more efficient.

3.3 Turbidity measurements

In situ UV-visible spectroelectrochemistry was employed to monitor and characterise the kinetics of growth using the same electrochemical thin layer cell. In this set-up the change in turbidity over time was a measure of the extent of polymer formation at the mesh electrode. The micro-mesh arrangement allowed optical transparency so the presence of any aggregated protein structures in the apertures, formed due to electrochemical reduction of O₂ *in situ*, could be detected as a result of wavelength independent light scattering caused by the polymers. The absorption spectroscopy technique permitted a more quantitative approach to monitoring growth compared with optical microscopy. Turbidity values are determined from the absorbance according to the relation $A = \log(I_0/I)$, where turbidity = (I_0/I) .

At a protein concentration of 300 mg cm⁻³ (the same as used in the optical microscopy experiments) large time dependent increases in turbidity were seen over the wavelength

range 600 to 1100 nm, Fig. 5. This wavelength-independent turbidity was directly due to light scattering caused by the formation of HbS aggregated structures. The blank in this experiment was the HbS solution before the potential was applied, so the spectra shown in Fig. 5 show the change in turbidity relative to the starting solution.

The rates of turbidity change at four wavelengths, 600 nm, 650 nm, 700 nm and 800 nm, were monitored as functions of time to investigate the kinetics of nucleation and growth, shown in Fig. 6.

The results showed that the rate of change in turbidity at each wavelength followed a sigmoidal pattern with an initial lag period up to 1000 s where little increase in turbidity was apparent (turbidity less than 2.00). This was followed by an exponential increase from 1000 s to 4500 s where the turbidity increased forty-fold to 85.36. These data were fitted to a model, section 3.4.

Control experiments were performed using HbA instead of HbS at the same concentration (300 mg cm⁻³) and solution conditions. No significant turbidity change was seen at the mesh electrodes especially at the wavelength range 650 nm to 1100 nm. There was a slight increase seen at 600 nm but this can be attributed to structural modifications due to the deoxygenation of the protein (Fig. 7A). No significant increases in turbidity were observed at 700 nm and 800 nm and there was no characteristic sigmoidal relationship (Fig. 7B). The change in turbidity at 700 nm for HbA (1.26 at 4500 s) was approximately forty six times lower than the turbidity measured for the same experiment with HbS in the cell (59.37 at 4500 s). In comparison to the HbS data, HbA controls provided strong evidence that any changes in turbidity with HbS were due to HbS aggregation and growth, induced through electrochemical deoxygenation.

3.4 Kinetics of polymerisation

Many studies have been devoted to investigate the kinetics of HbS polymerisation using a large variety of techniques,

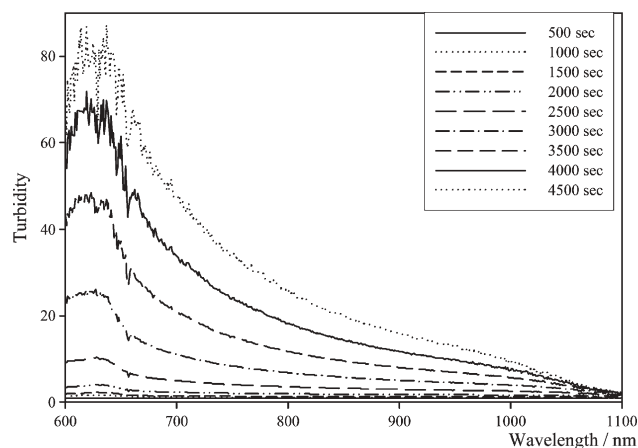


Fig. 5 Wavelength independent light scattering due to formation of HbS fibres by electrochemical reduction of oxygen at a Au micro-mesh electrode. The spectra (in the region 600–1100 nm) at regular times during the experiment are shown. Experiment conditions: HbS concentration 300 mg cm⁻³; 1.5 M pH 7.0 phosphate buffer; 0.5 M NaCl; $E = -0.55$ V vs. Ag/AgCl.

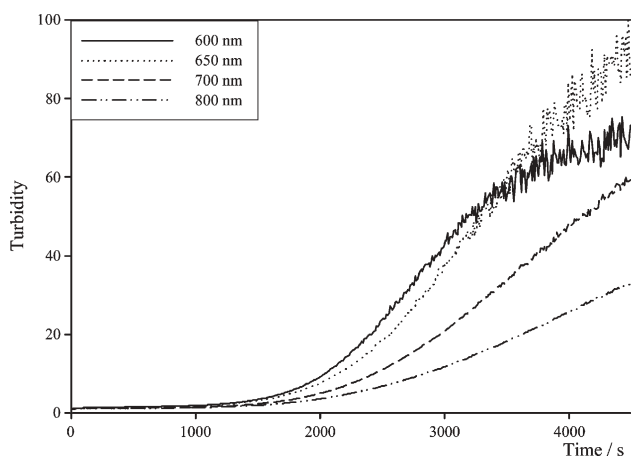


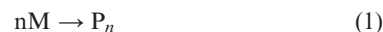
Fig. 6 UV-visible spectroelectrochemistry time traces for HbS showing changes in turbidity at Au micro-mesh electrode at specific wavelengths of 600, 650, 700 and 800 nm. Experiment conditions: HbS concentration 300 mg cm^{-3} ; 1.5 M pH 7.0 phosphate buffer; 0.5 M NaCl; $E = -0.55 \text{ V vs. Ag/AgCl}$.

including nuclear magnetic resonance,^{17,18} viscosity,^{19,20} turbidity,^{21,22} linear birefringence,^{23,24} light scattering^{25,26} and transverse relaxation times.²⁷ The results from all of these techniques have shown the same basic kinetic features of polymerisation, a sigmoidal time course for polymerisation of an initially polymer-free solution.

A marked delay in the initial part of the progress curve, during which no signal is observed, corresponds to the nucleation time or the time taken to form the critical nucleus. The energetic gain needed to form critical nuclei is dependent on the initial concentration of HbS. Furthermore, the nucleation time is also found to be related to the solubility of HbS, and thus dependent on the variables which alter the solubility of HbS such as the extent of deoxygenation, temperature, pH and ionic strength. Nucleation is followed by a comparatively fast and highly autocatalytic formation of polymer.^{28,29}

A kinetic scheme developed for the fibrillation mechanism of human calcitonin by Kamihira *et al.*³⁰ and subsequently modified for β -amyloid fibrillogenesis by Sabaté *et al.*³¹ was

fitted to our data. The kinetics of the process is controlled by two key parameters: the nucleation rate k_1 ,



and the growth described by the rate constant k_2 ,



with M representing monomeric HbS, n the number of HbS molecules and P_n the fibre nucleus. The overall kinetic equation for the nucleation and growth of the fibres can be expressed as in^{30,31}

$$\left(\frac{df}{dt}\right) = k_1(1-f) + k_2af(1-f) \quad (3)$$

where f is the fraction of fibres in the system and a is the initial concentration of HbS in the solution. Eqn (3) can be integrated under the boundary condition of $t = 0, f = 0$, to give

$$f = \frac{\rho\{\exp[(1+\rho)kt] - 1\}}{\{1 + \rho \exp[(1+\rho)kt]\}} \quad (4)$$

where $k = k_2a$ and $\rho = k_1/k$. We have used least squares fitting of eqn (4), to the turbidity data at 800 nm for two HbS concentrations to obtain values of k_1 and k_2 . As shown in Fig. 8 the fit of eqn (4) to the normalised turbidity data (normalised using a turbidity of 75, which was the maximum turbidity at 800 nm) is good for the high protein concentration data (300 mg cm^{-3} , $r^2 = 0.998$) but only reasonable for the lower protein concentration (50 mg cm^{-3} , $r^2 = 0.968$). The fit to the low protein concentration data was affected by solution evaporation from the cell which ultimately limited the length of the experiment to 4500 s. The rate constants obtained from these fits are summarised in Table 1. The effective growth rate constant, ak_2 , did not show significant correlation with HbS concentration under these conditions. However, the values for k_1 are several orders of magnitude smaller than k_2 for both 50 and 300 mg cm^{-3} of Hb, indicating that the nucleation process was far slower than the growth process. There was a clear concentration dependence on the nucleation rate constant.

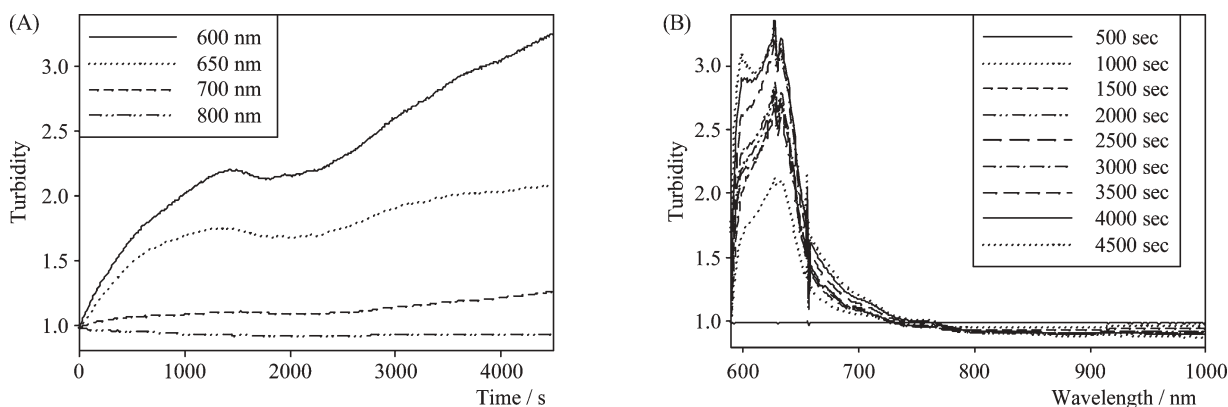


Fig. 7 (A) Wavelength independent light scattering due to HbA by electrochemical reduction of oxygen at a Au micro-mesh electrode. (B) UV-visible spectroelectrochemistry time traces for HbA showing changes in turbidity at a bare Au electrode. Experiment conditions: HbA concentration 300 mg cm^{-3} ; 1.5 M pH 7.0 phosphate buffer; 0.5 M NaCl; $E = -0.55 \text{ V vs. Ag/AgCl}$.

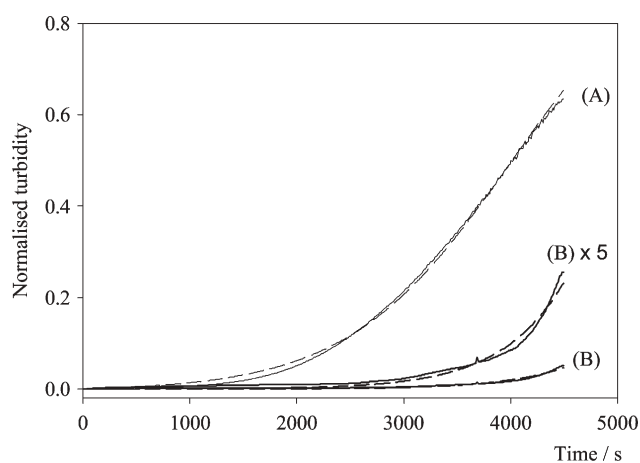


Fig. 8 Solid lines showing the experimental values of normalised turbidity using a maximum turbidity of 51 corresponding to maximum absorbance due to fibres at 800 nm, versus time for 300 mg cm⁻³ (A), and 50 mg cm⁻³ (B). The dashed lines are the best-fit lines to eqn (4).

Table 1 Nucleation rate constants k_1 and growth rate constants k_2 to describe the HbS fibre formation for two concentrations of protein. Experiment conditions: 1.5 M, pH 7.0 phosphate buffer; 0.5 M NaCl; temperature 25 °C; $E = -0.55$ V vs. Ag/AgCl for 4500 s

Concentration of HbS	k_1/s^{-1}	$k_2/M^{-1} s^{-1}$	ak_2/s^{-1}
50 mg cm ⁻³ (7.75×10^{-4} M)	$2.99 (\pm 0.4) \times 10^{-8}$	$1.39 (\pm 0.6)$	$1.08 (\pm 0.2) \times 10^{-3}$
300 mg cm ⁻³ (4.65×10^{-3} M)	$9.45 (\pm 0.08) \times 10^{-6}$	$0.26 (\pm 0.01)$	$1.22 (\pm 0.03) \times 10^{-3}$

This was expected, as in this case nucleation was expected to take place on the electrode surface where it is more thermodynamically favourable than homogenous nucleation.

4. Conclusions

It is demonstrated that polymerisation of HbS can be observed by oxygen depletion using electrochemical reduction in a thin layer cell. The extent of polymerisation was monitored using turbidity measurements at an optically transparent micro-mesh electrode. The change in turbidity was shown to be dependent on the HbS polymerisation and not protein precipitation, as shown by important control experiments replacing HbS for normal non-polymerising HbA. We show that the turbidity versus time traces fit the model for fibre formation described previously for human calcionin³⁰ and β -amyloid.³¹ Kinetic constants were determined for two concentrations of monomer, which showed that the nucleation rate was far slower than the growth, as expected. This method may not only be used to gain an understanding of the pathophysiology of sickle cell disease but also as a screening method for drugs that might lead to novel therapeutic strategies for disrupting nucleation and/or growth in patients with sickle cell crisis. This will be achieved by investigating the effect of new potential compounds, whose mode of action is

specific to the disruption of fibre formation, on the polymerisation of HbS in the electrochemical thin-layer cell.

Acknowledgements

ZI would like to thank EPSRC and the 'IRC in Nanotechnology' for a studentship. MAH is in receipt of a Programme Grant from The Wellcome Trust.

References

- L. Puling, H. A. Itano, S. J. Singer and I. C. Wells, *Science*, 1949, **111**, 543.
- V. M. Ingram, *Nature*, 1956, **178**, 792.
- G. Dykes, R. H. Crepeau and S. J. Edelstein, *J. Mol. Biol.*, 1979, **130**, 451.
- http://www.sicklecelldisease.org/about_scd/affected1.phtml.
- F. A. Ferrone, J. Hofrichter and E. A. Eaton, *J. Mol. Biol.*, 1985, **183**, 611.
- L. Sokolov and I. Mukerji, *J. Phys. Chem. B*, 2000, **104**, 10835.
- H. Wroblowa, Y. L. Pan and J. Razumney, *J. Electroanal. Chem.*, 1976, **69**, 195.
- W. A. Eaton and J. Hofrichter, *Adv. Protein Chem.*, 1990, **40**, 63.
- L. Stryer, *Biochemistry*, W. H. Freeman and Company, New York, 4th edn, 1995.
- R. W. Zurilla, R. K. Sen and E. Yeager, *J. Electrochem. Soc.*, 1978, **125**(7), 1103.
- Southampton Electrochemistry Group, *Instrumental Methods in Electrochemistry*, Ellis Horwood Limited, Chichester, 1993.
- D. Barham and P. Trinder, *Analyst*, 1972, **97**, 142.
- M. Kamihira, A. Naito, S. Tuzi, A. Y. Nosaka and H. Saito, *Protein Sci.*, 2000, **9**, 867.
- W. N. Poillon and J. F. Bertles, *J. Biol. Chem.*, 1979, **254**, 3462.
- <http://www.nlm.nih.gov/medlineplus/ency/article/003648.htm>.
- R. G. Bates, C. A. Vega and D. R. White, Jr, *Anal. Chem.*, 1978, **50**(9), 1295.
- G. C. Thompson, M. R. Waterman and G. L. Cottam, *Arch. Biochem. Biophys.*, 1975, **166**, 193.
- W. A. Eaton, J. Hofrichter, P. D. Ross, R. G. Tschudin and E. D. Becker, *Biochem. Biophys. Res. Commun.*, 1976, **69**, 539.
- K. Malfa and J. Steinhardt, *Biochem. Biophys. Res. Commun.*, 1974, **59**, 887.
- J. W. Harris and H. B. Bensusan, *J. Lab. Clin. Med.*, 1975, **86**, 564.
- J. G. Pumphrey and J. Steinhardt, *J. Mol. Biol.*, 1977, **112**, 359.
- H. R. Sunshine, J. Hofrichter and W. A. Eaton, *J. Mol. Biol.*, 1979, **133**, 435.
- J. Hofrichter, P. D. Ross and W. A. Eaton, in *Proceedings of the Symposium on Molecular and Cellular Aspects of Sickle Cell Disease*, publ. no. (NIH) 76-1007, DHEW, Bethesda, MD, 1976, p. 185.
- S. J. Gill, R. Spokane, R. C. Benedict, L. Fall and J. Wyman, *J. Mol. Biol.*, 1980, **140**, 299.
- J. G. Pumphrey and J. Steinhardt, *Biochem. Biophys. Chem. Commun.*, 1976, **69**(1), 99.
- S. Basak, F. A. Ferrone and J. T. Wang, *Biophys. J.*, 1988, **54**, 829.
- M. R. Waterman and G. R. Cottam, *Biochem. Biophys. Res. Commun.*, 1976, **73**, 639.
- J. Hofrichter, P. D. Ross and W. A. Eaton, Kinetic and thermodynamic investigation of deoxyhemoglobin S gelation, in *Proceedings of the First National Symposium on Sickle Cell Disease*, ed. J. I. Hercules, A. N. Schechter, W. A. Eaton, R. E. Jackson, DHEW publ. no. (NIH) 75, Bethesda, MD, 1974, p. 43.
- J. Hofrichter, P. D. Ross and W. A. Eaton, *Proc. Natl. Acad. Sci. U. S. A.*, 1974, **71**, 4864.
- M. Kamihira, A. Naito, S. Tuzi, A. Y. Nosaka and H. Saito, *Protein Sci.*, 2000, **9**, 867.
- R. Sabaté, M. Gallardo and J. Estelrich, *Biopolymers (Peptide Sci.)*, 2003, **71**, 190.